Metallomics

Integrated biometal science

www.rsc.org/metallomics

Volume 4 | Number 4 | April 2012 | Pages 317–390

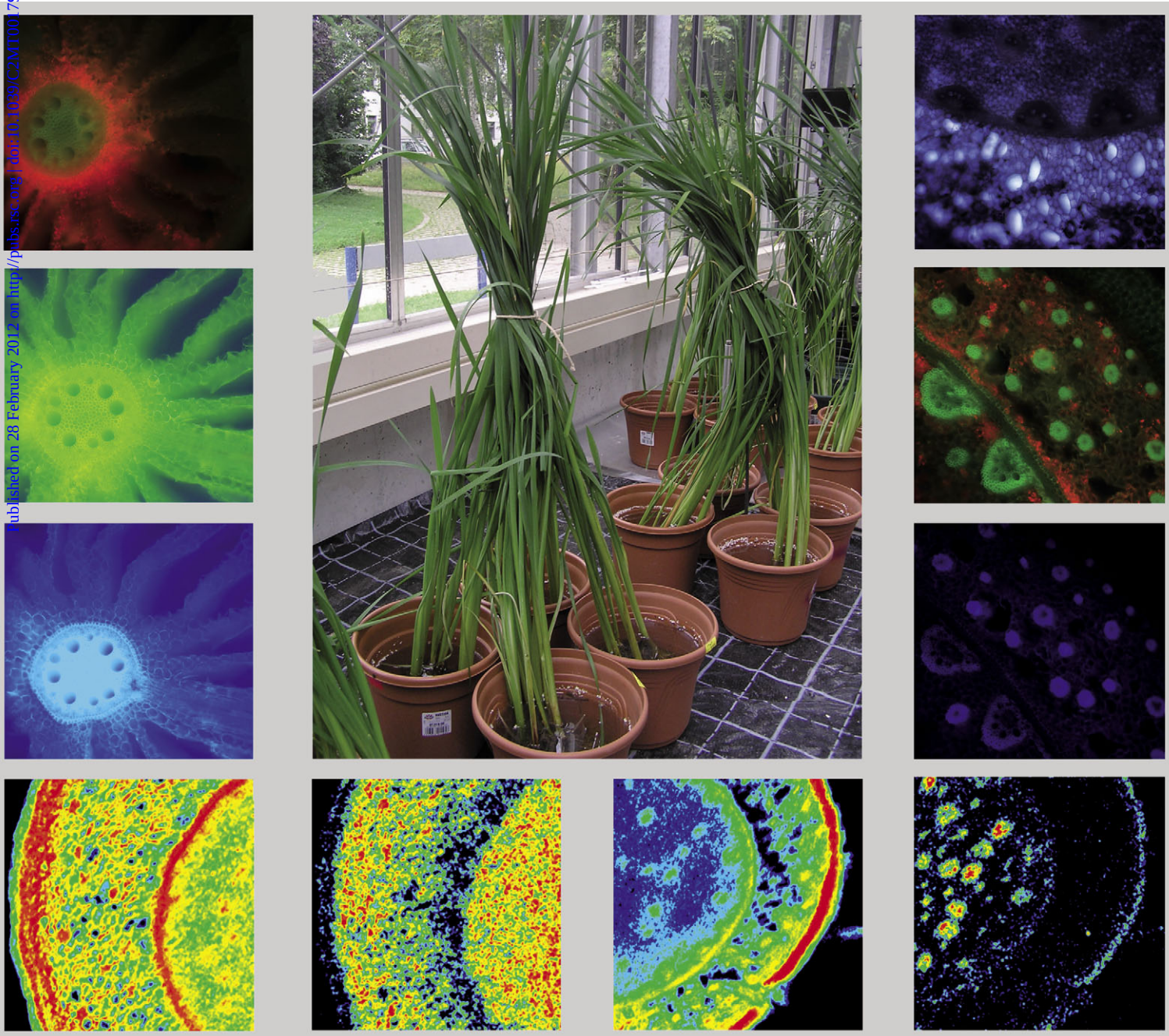

ISSN 1756-5901

RSC Publishing

PAPER

Lyubenova *et al.*

Localization and quantification of Pb and nutrients in *Typha latifolia* by micro-PIXE

Indexed in MEDLINE!

Metallomics

Dynamic Article Links
View Online

Cite this: *Metallomics*, 2012, **4**, 333–341

www.rsc.org/metallomics

PAPER

Localization and quantification of Pb and nutrients in *Typha latifolia* by micro-PIXE

Lyudmila Lyubenova,*[a] Paula Pongrac,[bc] Katarina Vogel-Mikuš,[b] Gašper Kukec Mezek,[c] Primož Vavpetič,[c] Nataša Grlj,[c] Peter Kump,[c] Marijan Nečemer,[c] Marjana Regvar,[b] Primož Pelicon[c] and Peter Schröder[a]

Received 15th November 2011, Accepted 3rd February 2012
DOI: 10.1039/c2mt00179a

Typha latifolia is a plant species widely used for phytoremediation. Accumulation, localization and distribution of Pb and mineral nutrients were investigated in roots, rhizomes and leaves of *Typha latifolia* grown at 0, 50, 100 and 250 μM Pb concentrations in a pot experiment under controlled conditions. Bulk elemental concentrations were determined by X-ray fluorescence (XRF) spectroscopy whereas micro-proton-induced X-ray emission (micro-PIXE) was used for element localization in root and rhizome tissues. Gradual increase in bulk Pb concentrations was observed in *Typha latifolia* roots and rhizomes treated with increasing Pb concentrations, however in rhizomes Pb concentrations were an order of magnitude lower than in roots. In leaves Pb concentrations were around the limit of detection for XRF ($\sim$20 μg g^{-1}). An increase in concentration of K and Ca in roots, rhizomes and leaves, of iron and zinc in roots and leaves, and of Mn in rhizomes was observed either at 50 and/or 100 μM Pb treatments, whereas for K and Ca in roots, rhizomes and leaves, Fe and Zn in roots and leaves and Mn in rhizomes, or at 250 μM Pb treatment the increase was seen for concentrations of Fe and Zn in rhizomes and Cu in roots. Mn concentrations decreased with Pb treatments in roots and leaves. Element localization using micro-PIXE analysis demonstrated Pb accumulation in epidermal and cortical tissues of treated roots and rhizomes, while in endodermis and vascular tissues Pb was not detected. A displacement of Ca from epidermal to cortical tissues was observed in Pb treated roots and rhizomes, pointing to cell wall immobilization of Pb as one of the tolerance mechanisms in *Typha latifolia*. High level of colocalization of Pb with P (r = 0.60), S (r = 0.37) and Zn (r = 0.70) was observed in Pb treated roots, while in rhizomes colocalization with the mentioned elements was still positive, but not that prominent. These results indicate that Pb may form complexes with phosphorus and sulfur compounds in roots and rhizomes, which may also represent attraction sites for binding Zn. Because of its large root and rhizome surface area acting as main sites for Pb adsorption, *Typha latifolia* may represent potentially efficient plant species for phytoremediation of Pb contaminated soils and waters.

1. Introduction

The mobilization of heavy metals from their natural reservoirs to the atmosphere, soil and water through mining and steel industry, transport activities, fertilizers and agrochemical applications is the most significant negative input of human activities on terrestrial and aquatic ecosystems.[1] Lead (Pb) is one of the main environmental concerns as it contaminates soil, groundwater and vegetation,[2] thus its removal from these systems is a subject of intense remediation research.

In plants increased Pb concentrations cause growth reduction and inhibition of cell division,[3] partially due to the changes in the water balance, hormonal status and membrane permeability.[4] Additionally, intense Pb uptake may impair plant mineral status by inhibiting the root uptake of essential cations (K, Ca, Mg, Mn, Zn, Cu, Fe) and some anions: *e.g.* nitrate (NO_3^-).[5] These mineral imbalances predominantly result from Pb induced disorders in the cell metabolism stemming from changes in the membrane transporter activities and the membrane structure.[5] Pb can physically block the access of various ions to the root absorption sites.[6] As a consequence,

[a] *Helmholtz Zentrum München, German Research Center for Environmental Health, Research unit Microbe-Plant Interactions, Ingolstädter Landstr. 1, D-85764 Neuherberg, Germany. E-mail: lyudmila.lyubenova@helmholtz-muenchen.de; Fax: +49 89 3187 3382; Tel: +49 89 3187 3541*
[b] *Department of Biology, Biotechnical Faculty, University of Ljubljana, Večna pot 111, SI-1000 Ljubljana, Slovenia*
[c] *Jožef Stefan Institute, Jamova 39, SI-1000 Ljubljana, Slovenia*

a decrease in concentrations of Ca, Mg, K and some other elements may be observed after exposure to Pb as in the case of *Zea mays* and *Cucumis sativus* roots.[7]

Pb is taken up from soil mainly into the root apoplast and accumulates near the endodermis where the casparian strip acts as the predominant Pb barrier restricting loading of Pb to the central cylinder and shoot transport, thus resulting in higher Pb root than shoot concentrations.[8–10] In the current literature, several reports on the Pb transport in terrestrial plants may be found,[11–13] whereas the information on Pb uptake and transport in aquatic and wetland plants is scarce. Due to the primary importance of wetland plant species for constructed wetlands, information on the uptake, transport and tolerance against Pb represent basis for their practical applications.

Typha latifolia is referred to as a Pb excluder,[14] meaning that Pb concentrations in leaves are maintained at constant low levels until critical soil concentrations are reached and toxicity ensues as a result of unrestricted metal transport.[15] Both, metal tolerance and metal exclusion ability of *T. latifolia* are believed to be related to its oxygen transport capability and the radial oxygen loss from the roots resulting in its ability to modify and immobilize metals already in the rhizosphere.[14] In comparison to several other Pb-tolerant plants *T. latifolia* was shown to have the highest impact on reduction of Pb contamination in real contaminated sites[16] pointing to high value of this plant species in phytoremediation of aquatic environments.

Bulk analyses of roots or shoots alone do not provide information on heavy metal tolerance as mechanisms of survival might be linked to particular tissues. This problem can easily be circumvented by using localization techniques that provide maps of lateral distribution of elements within the tissue. This is accessible by micro-proton induced X-ray emission (micro-PIXE), a highly sensitive localization technique yielding quantitative information on localization of elements in tissues with micrometre resolution.[17] Micro-PIXE has been efficiently used to determine spatial distribution of macro- and micro-nutrients and also of non-essential elements accumulated in excess.[18–21] It also enables the studies of elemental interactions[22] thus providing better understanding of the detoxification mechanisms and plant adaptations on heavy metal contaminated sites.

The main aims of the present study were therefore to shed more light on the uptake, translocation and localization of Pb in *T. latifolia* grown in the substrate with increasing Pb concentrations and to investigate the possible interactions of Pb with essential minerals. We hypothesised that (i) the majority of the Pb would be immobilized in the *T. latifolia* root epidermis and cortex, (ii) the amount of Pb in rhizomes and leaves would be much lower than that in the roots, and (iii) that Pb uptake would lead to repartition of certain major macro- and micro-nutrients within plant tissues.

2. Results

2.1. Bulk elemental concentration

Seven macro and micro-nutrients and Pb were detected in composite samples of different organs of *T. latifolia* treated with increasing concentrations of Pb (Table 1). Pb concentrations increased gradually with Pb treatment in roots and rhizomes, however for an order of magnitude lower Pb concentrations were found in rhizomes compared to those in roots. In shoots Pb concentrations were around the detection limit for XRF ($\sim$20 μg g^{-1}), therefore no distinct trends could be observed.

Concentrations of Cl were below the limit of detection for XRF in roots and rhizomes of all treatments, while Cl was detected in leaves with the highest concentration found at 100 μM Pb treatment. In comparison to the control an increase in K, Ca, Fe and Zn concentrations was observed at 100 μM Pb treatment in roots and leaves, while in rhizomes an increase in K and Ca was observed already at 50 μM Pb treatment. The highest Fe and Zn concentrations were found in rhizomes at 250 μM Pb treatment. Mn concentrations decreased with Pb treatments in roots and leaves, while in rhizomes they increased when compared to the controls. Cu concentrations in roots and leaves increased with increasing Pb concentrations, whereas in rhizomes they decreased. The results indicate that Pb treatment induced changes in the uptake of all of the measured mineral nutrients in *T. latifolia*.

Table 1 Bulk element concentrations (μg g^{-1}) in composite samples of roots, rhizomes and leaves of *Typha latifolia* treated with increasing concentrations of Pb (μM) obtained by X-ray fluorescence spectroscopy. C—control treatment. LOD—limit of detection (μg g^{-1}); data in square brackets denominate uncertainties of the measurement

	Roots				Rhizomes				Leaves			
Element (LOD)	C	50 Pb	100 Pb	250 Pb	C	50 Pb	100 Pb	250 Pb	C	50 Pb	100 Pb	250 Pb
Cl (6930)	<LOD	<LOD	<LOD	<LOD	<LOD	<LOD	<LOD	<LOD	23 400 [2720]	19 600 [3060]	24 400 [2800]	20 800 [2630]
K (1740)	8380 [764]	7830 [774]	10 500 [1140]	7430 [851]	18 000 [1040]	31 400 [1940]	29 200 [1880]	25 000 [1530]	39 500 [2100]	47 600 [2500]	49 700 [2540]	40 000 [2120]
Ca (1120)	10 500 [632]	13 200 [755]	14 200 [894]	12 000 [727]	5730 [413]	10 500 [782]	8700 [742]	7220 [576]	7360 [603]	8370 [684]	9760 [720]	6320 [561]
Mn (97.0)	327 [42]	261 [34.8]	199 [42.6]	151 [29.9]	<LOD	<LOD	271 [41.2]	118 [30.7]	512 [44]	310 [40.7]	404 [42.6]	447 [42.9]
Fe (64.0)	1740 [91]	1520 [79.5]	2920 [144]	2660 [127]	160 [20.4]	634 [47.7]	441 [36.3]	1530 [79.4]	171 [22.8]	168 [26.3]	201 [26.3]	120 [22.9]
Cu (27.0)	71.0 [13.4]	122 [12.6]	119 [15.3]	138 [11.4]	54.0 [8.9]	44.0 [12.7]	46.0 [10]	36.0 [9]	30.0 [7.6]	38.0 [10.4]	43.0 [9.3]	35.0 [9.4]
Zn (22.0)	683 [36.2]	1900 [88.5]	2210 [103]	1440 [66.5]	117 [10.1]	233 [17.7]	267 [16.5]	334 [19.2]	45.0 [6.65]	75.0 [10]	78.0 [8.8]	64.0 [8.6]
Pb (20.0)	543 [31.9]	6010 [272]	7290 [329]	12 300 [550]	29.8 [7.79]	596 [33.9]	825 [42.1]	1880 [87.7]	<LOD	<LOD	<LOD	<LOD

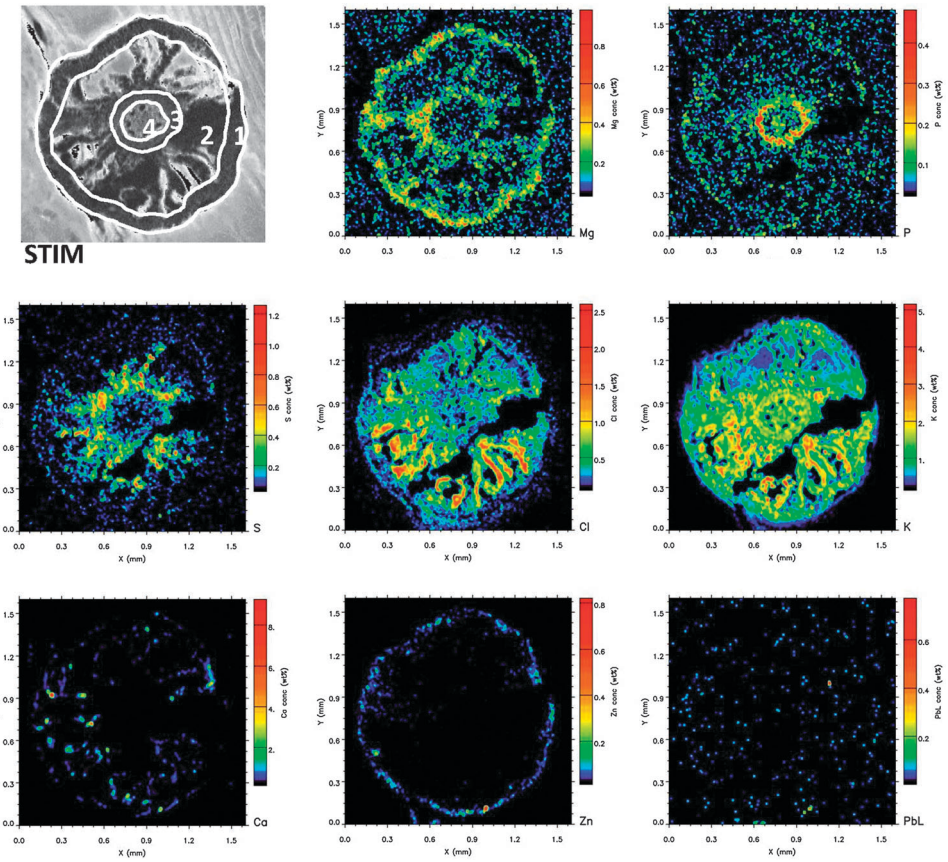

Fig. 1 Scanning transmission ion microscopy (STIM) image (upper left panel) with marked tissues recognised in roots (from left to right: 1—epidermis, 2—cortex, 3—endodermis, 4—vascular bundle) and quantitative elemental maps of Mg, P, S, Cl, K, Ca, Zn and Pb (as designated in the lower right corner of each subfigure) of a representative root cross-section of *Typha latifolia* grown in pots under controlled conditions. Scan size 1.5 × 1.5 mm^2.

2.2. Spatial distribution of elements

For the representation of the spatial distribution of elements in roots and rhizomes only the most extreme comparison of controls *vs.* plants treated with 250 μM Pb (Fig. 1–4) was selected. The roots and rhizomes from 250 μM Pb treatment showed the highest Pb concentrations and consequentially satisfactory statistics of Pb-L maps. Four different root tissues recognised in roots and five in rhizome maps are depicted in STIM maps (Fig. 1 and 3). Each tissue region was encircled, PIXE spectra were extracted from the encircled regions and finally quantitative analysis was performed by GUPIXWIN Software (Tables 2 and 3).

Pb was mainly localized in root epidermis of both control and treated plants (Tables 2 and 3; Fig. 1 and 2), and the concentrations of Pb in root tissues of treated plants were of three orders of magnitude higher than those of the controls (Table 2; Fig. 1 and 2). Despite high Pb concentration difference observed in epidermal root tissues between treated and control plants, Pb was not detected in endodermis and vascular bundles (Table 2). In rhizomes the concentration differences in epidermal tissues between both treatments were not that prominent. However, in control plants Pb was detected only in the epidermis of rhizome, while in treated plants Pb was also detected in hypodermis and cortex (Table 3). In vascular tissues Pb concentrations were below detection limits in both treatments (Table 3). In roots and rhizomes of plants treated with 50 and 100 μM Pb, a similar distribution pattern of Pb was seen as in 250 μM Pb treatment, with concentrations gradually decreasing from epidermis to vascular cylinder (data not shown). Plant treatment with Pb resulted in alteration of uptake, accumulation and distribution of mineral nutrients detected in roots and rhizomes. In roots an increase in epidermal and/or cortical concentrations of Mg, P, S, Cl, K, Ca, Zn, Mn and Fe of Pb treated plants was observed (Table 2). Concentrations of Si, S, Cl, K, Ca, Cu and Zn of Pb treated plants were also higher in endodermis and an increase of Si, P, Cl and S in vascular bundles was also noted. In rhizomes, the difference in Pb concentrations of treated plants was not that prominent when compared to the controls, with the exception of Mg, Si, P, S, Cl, K and Fe which significantly increased in epidermal and hypodermal tissues (Table 3) as also noticed from element distribution maps (Fig. 3 and 4).

Although absolute concentrations of Ca in roots and rhizomes were slightly higher in Pb treated plants than in controls (Tables 1–3), the ratios of Ca concentrations between cortical and epidermal tissues of roots and rhizomes increased significantly in Pb treated plants (from 1.8 in controls to 2.5 in Pb treated roots, and from 1.6 in controls to 3.9 in Pb treated rhizomes) (Tables 2 and 3). In addition a decrease in Ca concentration in epidermal tissues and an increase of Ca in cortical tissues of rhizome could be clearly seen in Pb treated plants when compared to the controls (Fig. 3 and 4).

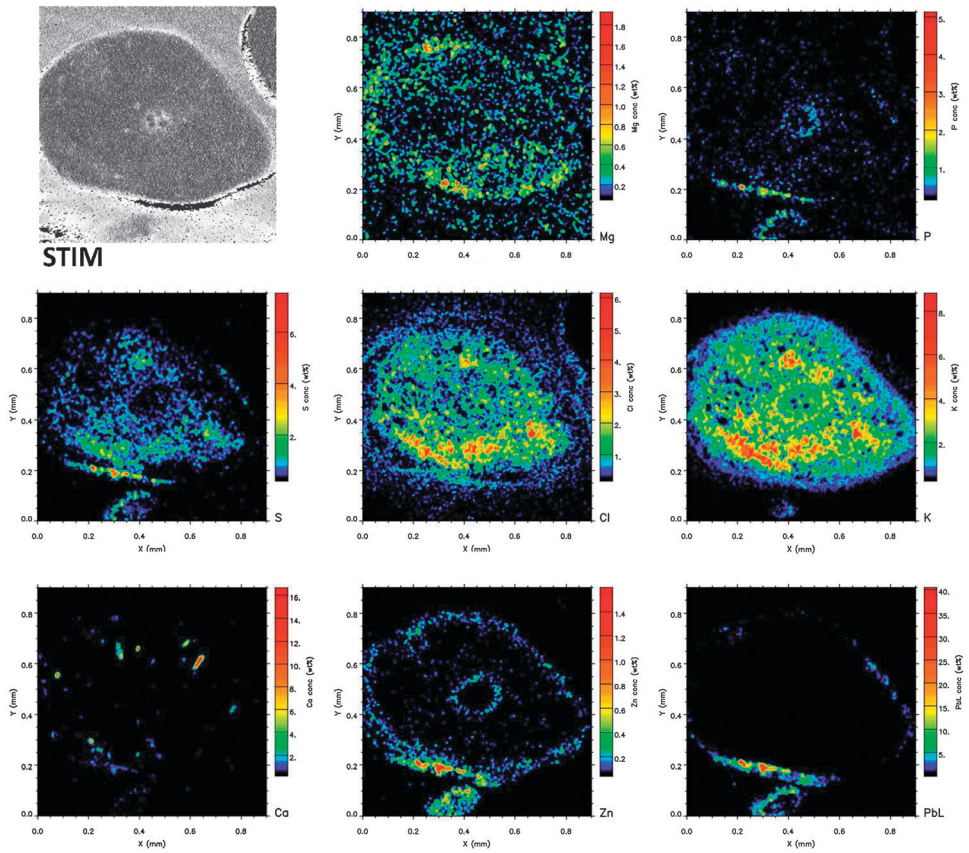

Fig. 2 Scanning transmission ion microscopy (STIM) image (upper left panel) and quantitative elemental maps of Mg, P, S, Cl, K, Ca, Zn and Pb of a representative root cross-section of *Typha latifolia* treated with 250 μM Pb in pots. Scan size 1.0 × 1.0 mm^2.

Taken together the results of Ca distribution in Pb treated roots and rhizomes indicate that Pb induced displacement of Ca from epidermal to cortical tissues.

Additional colocalization analysis performed on elemental maps produced by GEOPIXE II showed that Pb distribution in whole root cross-sections correlated well with distribution of P, S and Zn (Table 4), as also seen from Fig. 2, while in rhizomes correlation was still positive, but not that apparent (Table 4; Fig. 4). In whole root cross-section Mg, K and Ca showed slightly negative correlations with Pb while in rhizomes Pb correlation with Mg, Cl and K was positive and with Ca it was random (Table 4), clearly pointing to differences in Pb induced changes of nutrient accumulation between the two plant organs.

In the rhizodermis, the site of the most intensive Pb accumulation, highly positive correlations were observed between Pb and P, S, Cl and Zn (Table 4), while in cortex, where Pb concentrations were much lower, no distinct colocalization of Pb with other elements was observed. In epidermis of rhizomes the highest level of colocalization was observed between Pb and Zn, Cl, K and P, while in hypodermis the highest level of colocalization was observed between Pb and K, Zn, Ca and Cl.

3. Discussion

Wetland plants are generally not recognized as metal hyperaccumulators. If forced to take up metals, they store them preferentially in belowground organs, mainly roots and rhizomes.[23] This also applies for *T. latifolia*, since the highest concentrations of Pb were found in roots and for an order of magnitude lower concentrations were detected in the rhizomes as previously reported.[14] Pb concentrations in different organs of *T. latifolia* decreased in the order: roots > rhizomes ≫ leaves, pointing to an efficient Pb barrier within the roots. Similarly, decreasing concentrations in roots > leaves > stems > inflorescence > seeds, have been described[24] for other species, stressing the importance of the root barrier as a general root immobilization mechanism in plants.

In water hyacinth, most of the Pb was found to be concentrated in the inner root tissues.[25] On the other hand in mangrove plants, root epidermis seems to serve as a barrier for Pb transport towards aboveground tissues, but this does not apply for the other metals.[26] With development of modern quantitative element localization techniques such as micro-PIXE, which enables scanning of plant tissue samples with lateral resolution reaching one micrometre range, it became possible to localize the elements of interest and map their distribution in the inspected area. Using this method we have demonstrated that in *T. latifolia* Pb is mainly accumulated in epidermal tissues of roots and rhizomes of plants treated with 250 μM Pb, and Pb amounts progressively decrease towards the central core, where Pb concentrations were below the limit of detection for micro-PIXE (around 5 μg g^{-1}). These data can be related to findings that postulated precipitation of Pb in outer root tissues[27] limiting its penetration deeper within the plant tissues.

Considerable information is available on Pb distribution in the cells of terrestrial plants, but there are few such studies on aquatic plants. Ultrastructural studies have shown that in general Pb

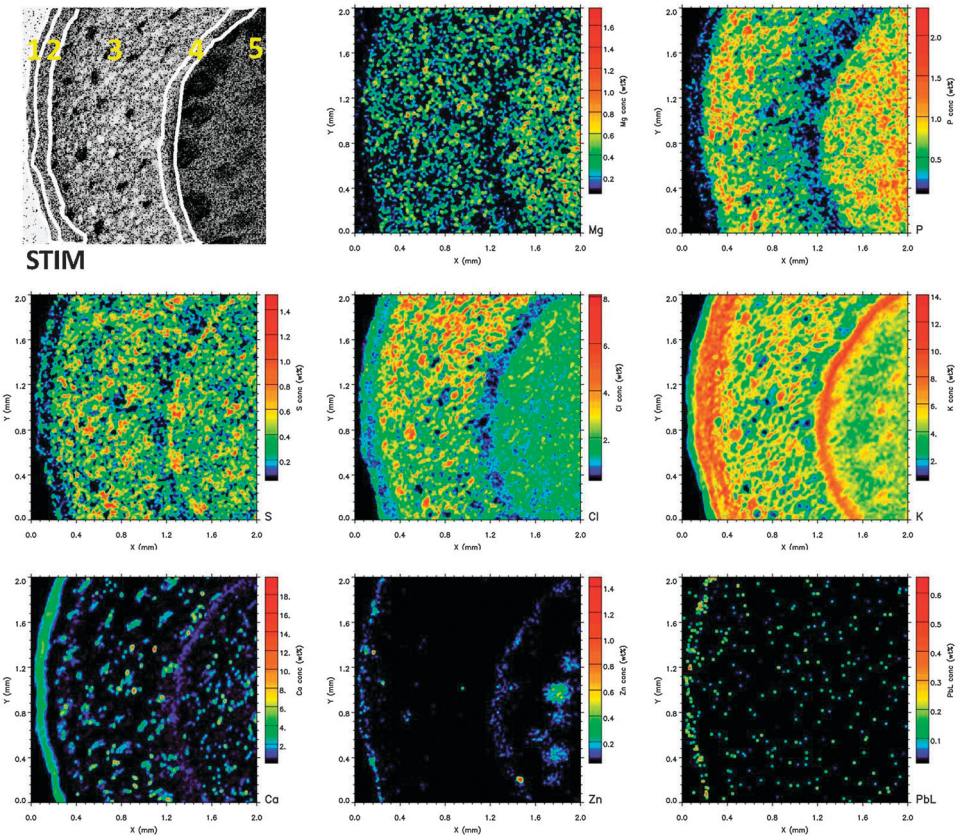

Fig. 3 Scanning transmission ion microscopy (STIM) image (upper left panel) with marked tissues recognised in rhizomes (from left to right: 1—epidermis, 2—hypodermis, 3—cortical region, 4—endodermis, 5—cental core) and quantitative elemental maps of Mg, P, S, Cl, K, Ca, Zn and Pb of a representative rhizome cross-section of *Typha latifolia* grown in pots under controlled conditions. Scan size 2.0 × 2.0 mm^2.

depots may be placed in the vacuoles, endoplasmatic reticulum, cell walls[4] and also cytoplasm.[28,29] The cell wall plays an important role in heavy metal tolerance by preventing toxic concentrations of metal ions from reaching sensitive sites[30] as shown for *Hylocomium splendens*[31] and a resistant clone of *Anthoxanthum odoratum*.[32] The plants' ability to accumulate Pb in the cell walls relies on their physical and chemical properties,[12] which can be altered in the presence of metals. Ions may accumulate predominantly in the matrix around the wall fibrils and this accumulation can lead to mineralization of the cell wall changing its physical and chemical properties.[27] In *Brassica juncea* it was demonstrated that Pb concentration at the root tip is more than threefold greater than that found in the mid-root region and ultrastructural examination suggested that observable quantities of Pb are not deposited in tissues internal to the casparian strip.[33] Similarly, our results showed that Pb deposition is largely extracellular, especially since a displacement of Ca from epidermal to cortical tissues was observed in roots and rhizomes. Because Pb has much higher affinity for binding to polycarboxylates, such as pectin, than Ca,[34] Pb probably induced a displacement of Ca from pectin bridges and bound to free carboxyl and hydroxyl groups generated after Ca displacement according to the "egg-box" model.[35] This could then prevent further diffusion of Pb into inner root or rhizome parts *via* the apoplast pathway and moreover this mechanism of locking of Pb into the cell wall could also prevent further diffusion of Pb toward the plasma membrane and Pb uptake into the root cell symplast.

A colocalization of P and S compounds and also Cl was observed at the sites of Pb accumulation, presumably due to the ability of Pb to form stable complexes with phosphates[28,36] and sulpfr compounds such as sulfates and thiols[36] in the cell walls, within the cells in the cytoplasm, and also in membrane bound vesicles and vacuoles.[28] In the presence of Pb some plants were shown to synthesize phytochelatins[37] and in Pb hyperaccumulating *Sedum alfredii* detoxification of Pb was related to glutathione.[38] In *T. latifolia* alteration in S metabolism in the presence of Pb was reflected also as an increase of S found in vascular tissues, probably phloem that could be related to mobilization of organic S compounds from shoots to the roots.

Similarly high colocalization of Pb with Zn in roots and an increase of Mg and K were observed in epidermal and hypodermal regions of rhizomes. This could probably be attributed to the cell wall modification caused by Pb treatment. An increase in number of free hydroxyl and carboxyl groups in the root and rhizome cell walls as a response to Pb treatment and displacement of Ca, and also accumulation of P, S and Cl ions and compounds in that region, would increase the possibility of binding also of other one and two-valent cations like Mg, K and Zn, besides Pb. Modification of the cell wall composition in the presence of Pb as well as alteration of membrane ion transport activities would also explain the overall increase of mineral concentrations in Pb treated plants, however further research is needed to confirm these very complex interactions between metal and plant cells and tissues.

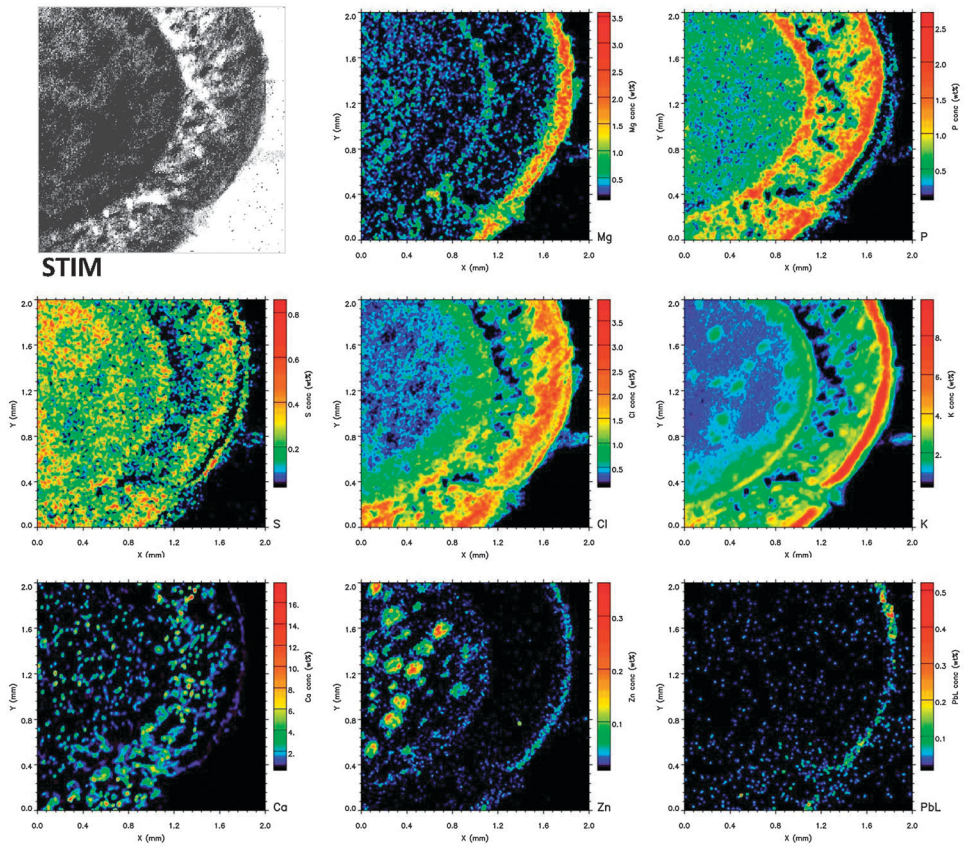

Fig. 4 Scanning transmission ion microscopy (STIM) image (upper left panel) and quantitative elemental maps of Mg, P, S, Cl, K, Ca, Zn and Pb of a representative rhizome cross-section of *Typha latifolia* treated with 250 μM Pb in pots. Scan size 2.0 × 2.0 mm^2.

Table 2 Element concentrations of representative selected regions within roots of *Typha latifolia* grown under controlled conditions (root control) and treated with 250 μM Pb (root 250 μM Pb) obtained by micro-PIXE. X-Ray spectra corresponding to particular root morphological structures were extracted from the encircled regions (as shown in STIM maps in Fig. 1) and analysed using GUPIX program. Error (%), uncertainty of the measurement; LOD, limit of detection (in μg g^{-1}); n.d., non-determined

	Epidermis			Cortex			Endodermis			Vascular bundle		
	μg g^{-1}	Error (%)	LOD	μg g^{-1}	Error (%)	LOD	μg g^{-1}	Error (%)	LOD	μg g^{-1}	Error (%)	LOD
Root control												
Mg	1460	6.80	165	1420	3.33	76.9	760	21.2	284.5	534	38.8	366
Si	829	3.76	52.1	334	5.15	29.9	295	23.7	124.7	LOD	—	148
P	339	9.36	57.6	333	6.47	39.3	2670	4.01	164	698	15.4	189
S	394	6.12	42.7	1360	1.74	40.2	1630	5.83	147.9	429	21.5	173
Cl	1340	1.95	37.1	6660	0.500	34.8	6130	2.12	149.2	3250	3.86	155
K	4520	0.88	33.6	21 500	0.290	29.0	35 000	0.88	154.4	21 900	1.42	179
Ca	1900	1.89	47.9	3380	1.78	101	2080	8.84	341.9	1240	13.7	311
Mn	21.6	13.6	5.3	14.5	20.3	5.30	54.8	26.3	21.2	n.d.	n.d.	n.d.
Fe	247	2.02	2.3	76.2	4.15	4.70	83.6	16.0	18.1	LOD	—	23.5
Cu	65.0	5.53	3.4	12.0	17.4	3.00	32.3	36.7	20.3	LOD	—	22.2
Zn	237	2.90	2.7	106	3.57	2.40	125	16.3	28.3	n.d.	n.d.	n.d.
Pb	25.5	33.7	11.4	15.4	41.0	8.40	n.d.	n.d.	n.d.	n.d.	n.d.	n.d.
Root 250 μM Pb												
Mg	2250	5.04	174	2210	5.83	207	964	31.4	514.2	n.d.	n.d.	n.d.
Si	466	9.60	78.5	715	9.69	119	961	16.1	257.5	1560	12.6	292
P	1340	4.84	108	1120	9.67	192	2830	8.47	375.9	1630	14.3	321
S	1490	6.25	201	12 700	1.30	222	6180	4.53	412	1470	14.2	300
Cl	5600	1.59	104	33 000	0.72	178	12 600	2.84	329.6	8670	3.74	241
K	19 400	0.81	101	89 600	0.48	204	52 900	1.46	402.9	17 000	2.94	360
Ca	3310	3.48	190	8370	3.81	584	4310	10.6	806.2	LOD	—	512
Mn	243	4.84	7.90	LOD	—	28.6	56.7	45.4	32.7	LOD	—	36.0
Fe	536	3.03	16.0	107	15.6	25.1	71.6	39.9	39.0	LOD	—	56.3
Cu	53.8	14.6	10.0	27.0	49.7	20.6	74.5	44.3	55.2	n.d.	n.d.	n.d.
Zn	1700	2.23	20.8	670	5.41	24.3	1720	7.67	60.7	LOD	—	82.9
Pb	13 200	1.82	125	362	19.5	87.6	n.d.	n.d.	n.d.	n.d.	n.d.	n.d.

Table 3 Element concentrations of representative selected regions within rhizomes of *Typha latifolia* grown under control conditions (rhizome control) and treated with 250 μM Pb (rhizome 250 μM Pb). X-Ray spectra corresponding to particular root morphological structures were extracted from the encircled regions (as shown in STIM maps of Fig. 3) and analysed using GUPIX program. Error (%), uncertainty of the measurement; LOD, limit of detection (in μg g^{-1}); n.d., non determined

	Epidermis			Hypodermis			Cortical region			Endodermis			Central core		
	μg g^{-1}	Error (%)	LOD	μg g^{-1}	Error (%)	LOD	μg g^{-1}	Error (%)	LOD	μg g^{-1}	Error (%)	LOD	μg g^{-1}	Error (%)	LOD
Rhizome control															
Mg	820	35.2	482	2260	8.07	301	2390	3.41	127.4	1200	17.9	364	4100	2.86	170.1
Si	250	38.6	166	237	27.1	111	179	17.9	54.2	LOD	—	141	252	16.9	72.0
P	1100	11.1	207	4770	1.97	135	5160	0.930	69.5	4550	2.50	164	7240	0.850	81.3
S	1380	8.20	195	2050	3.85	140	3240	1.53	86.1	3400	2.62	133	2540	1.73	71.2
Cl	12 000	1.53	157	17 400	0.690	104	25 100	0.290	56.5	9300	1.13	101	12 100	0.460	49.1
K	23 400	1.14	78.4	72 800	0.340	111	65 400	0.190	58.5	44 500	0.470	105	37 200	0.240	48.3
Ca	20 000	1.45	283	5580	3.56	359	8700	1.61	239.4	3450	4.23	267	4430	1.98	153.1
Mn	160	9.97	22.4	53.9	16.7	16.2	102	4.81	8.10	111	7.14	11.4	64.7	4.80	4.90
Fe	240	7.86	23.7	144	8.08	18.6	78.6	7.08	9.70	94.1	9.85	16.0	61.6	5.67	5.80
Cu	46.4	28.6	11.1	LOD	—	7.70	15.2	18.0	4.00	75.2	9.41	8.40	5.00	36.5	2.90
Zn	931	4.86	14.8	254	4.89	10.8	66.3	5.84	2.90	322	4.62	17.9	240	2.29	1.40
Pb	547	15.6	108	n.d.	n.d.	n.d.	LOD	—	10.2	n.d.	n.d.	n.d.	n.d.	n.d.	n.d.
Rhizome 250 μM Pb															
Mg	16 300	3.23	768	21 300	1.91	546	3520	1.91	102.7	5600	3.69	317	3050	1.86	86.4
Si	2600	5.04	215	1300	8.52	188	396	7.03	45.2	318	23.3	129	131	14.89	33.6
P	4230	3.42	233	5470	2.20	190	8740	0.470	55.4	11 600	0.950	141	4100	0.670	39.5
S	3260	3.61	196	1900	4.91	176	1540	1.98	54.9	2080	3.16	114	2010	0.980	30.2
Cl	17 600	0.930	147	16 900	0.69	123	12 200	0.300	32.9	9780	0.740	70.5	4090	0.470	21.4
K	64 800	0.470	134	1×10^5	0.23	73.5	30 600	0.180	35.6	30 000	0.370	51.7	9900	0.270	18.8
Ca	12 000	2.07	399	4690	5.41	486	18 600	0.450	111	5400	1.75	154	5800	0.570	44.4
Mn	85.4	10.1	13.3	31.2	20.9	12.0	14.3	16.26	4.3	46.6	7.62	5.9	17.9	6.82	2.1
Fe	393	3.66	12.7	166	5.49	13.6	70.2	3.99	4.7	94.5	4.48	5.4	61.2	2.35	2.1
Cu	58.8	14.8	9.80	12.5	29.9	5.50	LOD	—	3.1	14.3	16.27	2.7	6.3	13.66	1.4
Zn	444	4.97	14.6	123	6.22	7.40	59.5	3.72	2.2	121.7	4.31	4.2	238	1.2	1.1
Pb	535	11.7	73.4	47.7	31.9	21.3	31	18.79	9.7	n.d.	n.d.	n.d.	6.1	42.75	4.4

Table 4 Pearson's (*r*) correlation coefficients between Pb and other element concentrations measured in Pb treated *Typha latifolia* roots and rhizomes using micro-PIXE. Intensity correlation analysis was performed using "ImageJ" program. Zero–zero pixels are not included in this calculation. Colocalization analysis was performed only with those elements where statistics was sufficient to obtain element distribution maps (therefore Mn, Fe and Cu are not included). In particular tissues colocalization analysis was performed where sufficient Pb concentrations were detected (epidermis, hypodermis and cortex)

	Roots			Rhizomes		
Correlation	Whole crossection *r*	Epidermis	Cortex	Whole crossection *r*	Epidermis	Hypodermis
Pb–Mg	−0.19	−0.19	−0.01	0.40	0.22	−0.06
Pb–P	0.60	0.63	0.00	0.18	0.26	−0.08
Pb–S	0.37	0.75	−0.03	0.21	0.19	0.01
Pb–Cl	−0.09	0.38	0.00	0.25	0.27	0.17
Pb–K	−0.18	−0.11	0.00	0.26	0.27	0.20
Pb–Ca	−0.14	0.25	0.00	0.08	0.17	0.19
Pb–Zn	0.70	0.60	0.07	0.14	0.38	0.20

Despite the effective sequestration mechanisms which enable Pb immobilization in the cells of root and rhizome outer tissues, Pb concentrations in root and rhizome epidermal and cortical tissues increase with increasing Pb concentrations in medium, and it seems that the endodermis, a final suberized apoplastic barrier, represents the most important functional barrier of Pb transport into the central cylinder and further to the shoots. Similar results have been found also in some dicotyledonous species and in maize.[39–42]

4. Experimental section

4.1. Plant samples

Typha latifolia plants were obtained from a local plant distributor (Jörg Petrowsky, D-29348 Eschede, Germany) in 9 × 9 cm pots; the roots were cleaned from the soil and planted in 5 L pots filled with perlite, where the plants were grown for 52 days under greenhouse conditions in Helmholtz Zentrum, München, Germany as follows: relative humidity of 60% (day) and 70% (night), *T* 20 °C (day) and *T* 15 °C (night) and 12 daylight hours. The nutrient solution was 10 g Murashige and Skoog medium (Duchefa) in tap water, added to pots once per week.[43]

4.2. Lead treatment

After the establishment of plants for 53 days in perlite, plants were watered with 0, 50, 100 and 250 μM $PbCl_2$ added to the nutrient solution and grown in the chambers for next 7 days. At the end of the treatment the plants were transported to the

laboratory in Ljubljana, Slovenia, where they were kept in growth chambers until harvest and sample preparation.

4.3. Plant bulk elemental analyses

After a careful wash in tap and distilled water three *T. latifolia* plants per Pb treatment/concentration were sampled for micro-PIXE analysis. The rest of the plants were separated into roots, rhizomes and leaves and oven-dried (60 °C) for 48 h. The dried material was pulverised in liquid nitrogen and pressed into pellets. Concentrations of Cl, K, Ca, Mn, Fe, Cu, Zn and Pb in composite samples were determined by X-ray fluorescence (XRF) spectroscopy using a Cd-109 radioisotope excitation source.[44] Mg, Si, P and S were below the detection limit for XRF. Standard reference material Tomato leaves 1573a with certified concentrations of minerals was used for quality assurance of elemental analysis.

4.4. Sample preparation for micro-PIXE analysis

The roots were detached from the intact plants, quickly washed in deionised water and sectioned with a razor blade to shorter pieces (2 cm from the root tip). The pieces were immediately transferred into Al beds filled with tissue freezing medium (Jung, Leica) and dipped into liquid nitrogen.[16] Root pieces were sectioned with a Leica CM3050 cryotome (Leica, Bensheim, Germany) at temperatures between −25 °C and −20 °C to 60 μm thick sections. The sections were then placed in specially designed Al holders with a heavy cover to ensure the flatness of the sections during drying. The rhizome was manually cut with a razor blade to thin slices, put into Al beds and immediately frozen in liquid nitrogen. The holders with root cross-sections and Al beds with rhizome cross-sections were then transferred to an Alpha 2–4 Christ freeze dryer *via* a cryo-transfer-assembly cooled by liquid nitrogen and freeze-dried at −25 °C and a pressure of 0.384 mbar for two days. Freeze-dried root and rhizome cross-sections were mounted on Al sample holders between two thin layers of Pioloform foil.[17,45]

4.5. Micro-proton induced X-ray emission analysis

Micro-PIXE analysis was performed with the nuclear microprobe of the Jožef Stefan Institute[46,47] on 3 different samples per treatment. A proton beam energy of 3 MeV was used in order to get an optimal signal to background ratio for the elements with Z over 30. Beam intensity was determined by the total count rate of the system, which was kept below 800 Hz to avoid excessive dead times in the data acquisition system. Under such conditions, beam diameter was kept well below 2 micrometres and beam intensity below 400 pA. Simultaneously an on–off axis scanning transmission ion microscopy[48] (STIM) was performed to determine beam exit energy from the sample, related to the sample local areal density. In combination with known matrix composition, proton exit energy measured by STIM was used for determination of specimen thickness. Precision of proton exit energy measurements with STIM was in the order of 10 keV. The energy loss in *Typha latifolia* samples was in the range between 120 and 300 keV. This reflects the precision of sample thickness determination of better than 8%.

A pair of X-ray detectors was used to efficiently cover the energy range from 0.8 keV up to 30 keV, and electron spraying of the sample during the analysis was used to prevent against sample charging.[18] Proton dose was measured with a beam chopper positioned after the collimating slits.[20]

X-Ray and STIM spectra corresponding to distinct morphological structures of roots and rhizomes (Fig. 1 and 3) were extracted from the analysed regions of the samples (Tables 2 and 3). Assuming a cellulose matrix and the proton exit energy measured by STIM, the elemental concentrations were calculated using GUPIXWIN program.[49]

For the generation of the elemental images dynamic analysis methods were used,[50,51] which are an essential part of GEOPIXE II software package. The advantages of the code are deconvolution of background and X-ray line overlapping for the imaging presentation of the elemental maps. An identical matrix composition (cellulose $C_6H_{10}O_5$) was assumed in each pixel of mapped areas. The image of each element was based on a group of X-ray lines (typically K or L lines).[19] Images of Mg, P, S, Cl, K, Ca and Zn were obtained from K lines, whereas L lines were used for Pb imaging. For Si, Mn, Fe, Ni and Cu the statistics of counts was too low to obtain decent maps. The calibration of the PIXE method is periodically checked by the analysis of the multi-elemental standard reference materials NIST SRM 1573a (Tomato leaves, homogenized powder, analysed in the form of a pressed pellet), NIST SRM 1107 (Naval Brass B, alloy) and NIST SRM 620 (Soda-Lime Flat Glass), series of monoelemental metals in the form of bulk and thin foils.

4.6. Colocalization analysis

Colocalization analysis of Pb distribution with other elements obtained by micro-PIXE mapping was performed by ImageJ program using plug-in "Intensity correlation analysis", generating Pearson's correlation coefficients (r) (http://www.Macbio-photonics.ca/imagej/colour_analysis.htm). Quantitative, 512 × 512 pixel, 8-bit, colour elemental maps generated by GEOPIXE II were used for colocalization analysis. Pearson's correlation coefficients range from 1 to −1, where a value of 1 represents perfect correlation/colocalization; a value of −1 represents perfect exclusion, and zero represents random localization.

5. Conclusion

Results indicate that the casparian strip represents the main barrier for apoplastic Pb penetration into the root and rhizome vascular tissues of *T. latifolia*. However, most of the Pb actually accumulates in the cells of epidermal and cortical tissues and does not pass deeper or further towards the central core. Clearly, more information about mechanisms of metal uptake, distribution and removal by wetland species is urgently required in order to ensure that the wetlands themselves do not become sources of metal contamination to surrounding areas.[23]

According to our findings, *T. latifolia* has potential for removing Pb from contaminated substrates due to its large root and rhizome surface area, making it suitable plant species for rhizofiltration. The next investigation step on Pb uptake by this plant will involve treatments with multi-metal contamination

and should focus on the enhancement of uptake by identifying proteins responsible for the transport of metals across the plasma membrane and controlling their expression as well as resolving the role and modification of the cell wall components in the presence of Pb.

Abbreviations

XRF	X-ray fluorescence
micro-PIXE	micro-proton-induced X-ray emission
STIM	scanning transmission ion microscopy

Acknowledgements

This work has been supported by the European Community as an Integrating Activity 'Support of Public and Industrial Research Using Ion Beam Technology (SPIRIT)' under EC contract no. 227012. Support of Slovenian Research Agency of the research project J7-0352, research programs P1-0112, P1-0212 and research infrastructure of Microanalytical centre is acknowledged.

References

1 L. R. Lado, T. Hengl and H. I. Reuter, *Geoderma*, 2008, **148**, 189–199.
2 J. W. Huang, J. Chen, W. R. Berti and S. D. Cunningham, *Environ. Sci. Technol.*, 1997, **31**, 800–805.
3 F. A. Bazzaz, R. W. Carlson and G. L. Rolfe, *Physiol. Plant.*, 1975, **34**, 326–329.
4 P. Sharma and R. S. Dubey, *Braz. J. Plant Physiol.*, 2005, **17**, 35–52.
5 A. Kabata-Pendias and H. Pendias, *Trace Elements in Soils and Plants,* CRC Press, Boca Raton, London, 2nd edn, 1992, p. 365.
6 D. L. Godbold and C. Kettner, *Plant Physiol.*, 1991, **139**, 95–99.
7 W. M. Walker, J. E. Miller and J. J. Hassett, *Soil Sci.*, 1977, **124**, 145–151.
8 S. Verma and R. S. Dubey, *Plant Sci.*, 2003, **164**, 645–655.
9 I. V. Seregin and V. B. Ivanov, *Fiziol. Rast.*, 1997, **44**, 915–921.
10 I. V. Seregin and V. B. Ivanov, *Russ. J. Plant Physiol.*, 2001, **48**, 523–544.
11 M. Wierzbicka, *Environ. Exp. Bot.*, 1994, **34**, 173–180.
12 M. Wierzbicka, *Plant Sci.*, 1998, **133**, 105–119.
13 S. O. Eun, H. S. Youn and Y. Lee, *Physiol. Plant.*, 2000, **110**, 357–365.
14 Z. H. Ye, A. J. M. Baker, M. H. Wong and A. J. Willis, *New Phytol.*, 1997, **136**, 469–480.
15 A. J. M. Baker, *J. Plant Nutr.*, 1981, **3**, 643–654.
16 C. Lan, G. Chen, L. Li and M. H. Wong, *Environ. Manage.*, 1992, **16**, 75–80.
17 K. Vogel-Mikuš, P. Pongrac, P. Pelicon, P. Vavpetič, B. Povh, H. Bothe and M. Regvar, *Symbiotic Fungi: Principles and Practice*, 2009, vol. 18, pp. 227–242.
18 K. Vogel-Mikuš, J. Simčič, P. Pelicon, M. Budnar, P. Kump, M. Nečemer, J. Mesjasz-Przybylowicz, W. J. Przybylowicz and M. Regvar, *Plant, Cell Environ.*, 2008a, **31**, 1484–1496.
19 K. Vogel-Mikuš, M. Regvar, J. Mesjasz-Przybylowicz, W. J. Przybylowicz, J. Simčič, P. Pelicon and M. Budnar, *New Phytol.*, 2008b, **179**, 712–721.
20 K. Vogel-Mikuš, P. Pelicon, P. Vavpetič, I. Kreft and M. Regvar, *Nucl. Instrum. Methods Phys. Res., Sect. B*, 2009a, **267**, 2884–2889.
21 A. G. Kachenko, B. Singh, N. P. Bhatia and R. Siegele, *Nucl. Instrum. Methods Phys. Res., Sect. B*, 2008, **266**, 667–676.
22 P. Pongrac, K. Vogel-Mikuš, P. Vavpetič, J. Tratnik, M. Regvar, J. Simčič, N. Grlj and P. Pelicon, *Nucl. Instrum. Methods Phys. Res., Sect. B*, 2010, **268**, 2205–2210.
23 J. S. Weis and P. Weis, *Environ. Int.*, 2004, **30**, 685–700.
24 D. M. Antosiewicz, *Acta Soc. Bot. Pol.*, 1992, **61**, 281–299.
25 P. A. Vesk, C. E. Nockolds and W. G. Allaway, *Plant, Cell Environ.*, 1999, **22**, 149–158.
26 G. R. MacFarlane and M. D. Burchett, *Mar. Environ. Res.*, 2002, **54**, 65–84.
27 A. Frey-Wyssling, *JAWA Bull.*, 1982, **31**, 25–30.
28 P. M. Kopittke, C. J. Asher, F. P. C. Blamey, G. J. Auchterlonie, Y. N. Guo and N. W. Menzies, *Environ. Sci. Technol.*, 2008, **42**, 4595–4599.
29 S. Samardakiewicz and A. Wozny, *Plant Soil*, 2000, **226**, 107–111.
30 D. A. Thurman, *Effect of Heavy Metal Pollution on Plants,* Applied Science Publishers, 1981, vol. 2, pp. 239–249.
31 B. M. Gullvag, H. Skaar and E. M. Ophus, *J. Bryol.*, 1974, **8**, 117–122.
32 J. A. Qureshi, K. Hardwick and H. A. Collin, *J. Plant Physiol.*, 1986, **122**, 357–364.
33 D. E. R. Meyers, J. A. Graeme, I. W. Richard and B. Wood, *Environ. Pollut.*, 2008, **153**, 323–332.
34 V. M. Dronnet, C. M. G. C. Renard, M. A. V. Axelos and J. F. Thibault, *Carbohydr. Polym.*, 1996, **30**, 253–263.
35 E. R. Morris, D. A. Rees, D. Thom and J. Boyd, *Carbohydr. Res.*, 1978, **66**, 145.
36 S. Tian, L. Lu, X. Yang, S. M. Webb, Y. Du and P. H. Brown, *Environ. Sci. Technol.*, 2010, **44**, 5920–5926.
37 S. Andra, R. Datta, D. Sarkar, S. Bach and C. Mullen, *Plant Soil*, 2009, **326**, 171–185.
38 D. K. Gupta, H. G. Huang, X. E. Yang, B. H. N. Razafindrabe and M. Inouhe, *J. Hazard. Mater.*, 2010, **177**, 437–444.
39 M. Wierzbicka, *Plant, Cell Environ.*, 1987, **10**, 17–26.
40 G. Tung and P. J. Temple, *Sci. Total Environ.*, 1996, **188**, 71–85.
41 S. D. Lane and E. S. Martin, *New Phytol.*, 1977, **79**, 281–286.
42 W. F. Punz and H. Sieghardt, *Environ. Exp. Bot.*, 1993, **33**, 85–95.
43 T. Murashige and F. Skoog, *Physiol. Plant.*, 1962, **15**, 473–497.
44 M. Nečemer, P. Kump, J. Ščančar, R. Jačimović, J. Simčič, P. Pelicon, M. Budnar, Z. Jeran, P. Pongrac, M. Regvar and K. Vogel-Mikuš, *Spectrochim. Acta, Part B*, 2009, **63**, 1240–1247.
45 T. Schneider, S. Sheloske and B. Povh, *Int. J. PIXE*, 2002, **12**, 101–107.
46 J. Simčič, P. Pelicon, M. Budnar and Ž. Šmit, *Nucl. Instrum. Methods Phys. Res., Sect. B*, 2002, **190**, 283–286.
47 P. Pelicon, J. Simčič, M. Jakšič, Z. Medunic, F. Naab and F. D. McDaniel, *Nucl. Instrum. Methods Phys. Res., Sect. B*, 2005, **231**, 53–59.
48 J. Pallon, V. Auzelyte, M. Elfman, M. Garmer, P. Kristiansson, K. Malmqvist, C. Nilsson, A. Shariff and M. Wegden, *Nucl. Instrum. Methods Phys. Res., Sect. B*, 2003, **219**, 988–993.
49 J. L. Campbell, T. L. Hopman, J. A. Maxwell and Z. Nejedly, *Nucl. Instrum. Methods Phys. Res., Sect. B*, 2000, **170**, 193–204.
50 C. G. Ryan and D. N. Jamieson, *Nucl. Instrum. Methods Phys. Res., Sect. B*, 1993, **77**, 203–214.
51 C. G. Ryan, D. N. Jamieson, C. L. Churms and J. V. Pilcher, *Nucl. Instrum. Methods Phys. Res., Sect. B.*, 1995, **104**, 157–165.